Surface Oxidation of Liquid Sn[†]

Alexei Grigoriev [a, ††], Oleg Shpyrko [b], Christoph Steimer [a], Peter S. Pershan [a,b], Benjamin M. Ocko [c], Moshe Deutsch [d], Binhua Lin [e], Mati Meron [e], Timothy Graber [e], and Jeffrey Gebhardt [e]

[a] *Division of Engineering and Applied Sciences, Harvard University, Cambridge, Massachusetts 02138, USA*
[b] *Department of Physics, Harvard University, Cambridge, Massachusetts 02138, USA*
[c] *Department of Physics, Brookhaven National Lab, Upton, New-York 11973, USA*
[d] *Department of Physics, Bar-Ilan University, Ramat-Gan 52900, Israel*
[e] *The Consortium for Advanced Radiation Sources, The University of Chicago, Chicago, Illinois 60637, USA*

Introduction

Chemical reactions at interfaces are of the fundamental and practical scientific interest. They sometimes exhibit both unusual kinetics and new phases that are unstable in the bulk [1,2]. In spite of the fact that the free surfaces of liquid metals have recently attracted considerable attention because of the atomic ordering at the liquid-vapor interface [3] there have been very few studies of their reactive properties [4,5]. Oxidation of such surfaces are of particular interest because they lack the types of defects at which homogeneous nucleation occurs on solid surfaces namely steps, pits and dislocations [1]. In addition, surface oxidation of liquid metals can drastically change the surface tension which will have a profound effect on the way the liquid metal wets different surfaces [6]. This is important for practical processes such as soldering, brazing, casting etc.

The only two liquid metals for which the structure of the surface oxide has been studied by x-ray scattering technique are In and Ga, which were found to behave differently [4,5]. In the present report we present both x-ray reflectivity and GID studies of the oxide growth on the liquid Sn surface. In addition to the static features of the structure, these measurements also provide important information on the oxidation kinetics of the liquid Sn surface.

Experimental Details

The measurements presented here were carried out at ChemMatCARS 15-ID-C experimental station of the Advanced Photon Source at Argonne National Lab at an x-ray wave-length of 1.1273Å (11.0 KeV). A Sn sample of 99.9999% purity was placed in a molybdenum pan (diameter ~60 mm) and heated under UHV conditions to $240^0 C$ just above the Sn melting point $T_m = 232^0 C$. The vacuum in the baked out chamber was in the 10^{-10} Torr range and the oxygen partial pressure was below 10^{-11} Torr. Native oxide present in the original sample was removed by a combination of mechanical scraping and sputtering with Ar^+ ions.

The study of atomically clean liquid Sn surface [3] was followed by controlled oxidation of the cleaned Sn sample through introduction of ultra-high purity research grade oxygen gas (99.9999% purity, Matheson Tri-Gas Inc.)

[††] Corresponding author. *Present address:* University of Wisconsin-Madison, 1509 University Avenue, Madison, WI 53706, *Phone:* 608/262-7433, *E-mail address:* alexey@cae.wisc.edu
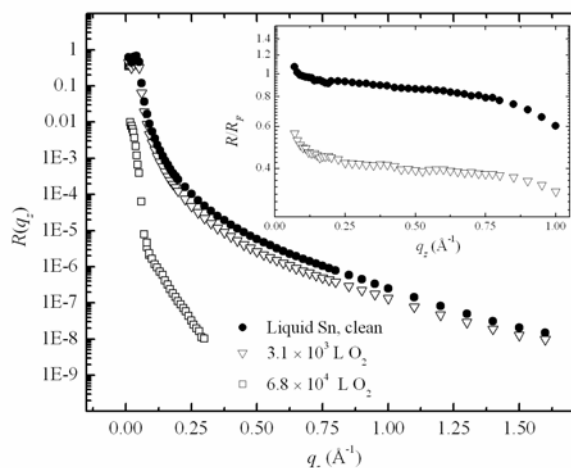
Fig. 1. X-ray reflectivity of the clean liquid Sn surface (•) (step #0); the surface after an oxygen dose of 3.1×10^3 L at an oxygen partial pressure 2×10^{-5} Torr (∇) (step #3) and after the complete oxidation of the surface ($\square$) (step #8). The inset shows the measured reflectivities normalized by the Fresnel reflectivity.

through a leak valve. The oxidation was done in several steps by exposing the UHV chamber to selected oxygen pressures for fixed time intervals. After obtaining the desired dosages the oxygen was pumped out of the chamber and measurements were carried out in an oxygen-free environment.

Results and Discussion

Specular x-ray reflectivity scan was taken prior to oxidation, then measured again after the total oxygen exposures of 3.1×10^3 L, and finally after the complete oxidation of the sample, when the surface visually appeared to be heavily oxidized. These results are shown in Fig. 1. The inset of Fig. 1 displays the same data normalized by the Fresnel reflectivity, $R_f(q_z)$, for pure Sn. In addition to these reflectivity scans the reflected signal at the point corresponding to the specular condition at $q_z = 0.5$ Å^{-1} was continuously monitored during the entire oxidation process even when the Sn surface was heavily oxidized and the specular signal was smeared out.

Fig. 1 depicts the reflectivity from the clean and oxidized surface of liquid Sn. The inset shows that for $q_z < 1$ Å^{-1} the specular x-ray reflectivity recorded from the oxidized sample has essentially the same shape as that of the unoxidized clean

Sn surface. This result allows us to conclude that the oxidation effect at this oxidation step is to *homogeneously* reduce the reflectivity for $q_z < 1$ Å^{-1} by a factor of ~0.45. The simplest explanation that would account for this is that the oxidation proceeds by formation of oxide patches which coexist with clean Sn surface patches in a way similar to that observed for liquid Ga [7]. With this interpretation about 55% of the surface would be coated by a non-reflecting oxide layer, while the remaining 45% would be clean liquid Sn patches.

Small angle off-specular diffuse scattering data (not shown here) make a correction to the interpretation given above. The correction is that the reflected x-ray signal is attenuated not only due to the oxide blocking a reflection from the clean surface but also due to deviations in the local curvature of the sample surface as a result of oxidation. By this interpretation the fraction of the surface that is actually oxidized must be less than ~55%.

Regardless of whether or not exactly 55% of the surface is oxidized after the total exposure of 3.1×10^3 L it is reasonable to suggest that the specular reflectivity at some fixed q_z is proportional to the fraction of the surface that is coated with oxide. The data in Fig. 2 show the signal at $q_z = 0.5$ Å^{-1} as a function of time during the oxygen exposure. The inset of Fig. 2 shows the slopes, which we designate as our "oxidation rate", as a function of the oxygen pressure. This "oxidation rate" clearly shows a monotonic dependence on the oxygen pressure, as well as a clear oxidation threshold pressure of ~5×10^{-6} Torr.

The detailed analysis of the oxidation kinetics allowed us to propose that the threshold for homogeneous oxidation of the liquid Sn surface falls within the pressure range of 3.0×10^{-6} Torr and 6.2×10^{-6} Torr.

The structure of the Sn surface oxide was probed by GID measurements. The results for the liquid Sn surface before oxidation and after an exposure of 4000 L are presented in Fig. 3 together with a plot of the difference between the two. In addition, simulated diffraction patterns of known Sn oxide structures are presented in Fig. 3 below the experimental data. The broad peak around $q_{xy} = 2.234$ Å^{-1} corresponds to the bulk liquid structure of Sn and is in good agreement with published data [8]. The two sharp oxide peaks appear at $q_{xy} = 2.442$ Å^{-1} and 2.827 Å^{-1}. No other peaks were observed in the accessible range $0 \leq q_{xy} \leq 3.2$ Å^{-1}. The positions of the observed peaks change with q_z and follow the powder diffraction pattern cone. This result indicates that the new peaks appeared as a result of the Sn surface oxidation formation of a three dimensional powder crystal structure.

The two most likely surface oxides expected for Sn are SnO and SnO$_2$, which are the only bulk oxides of Sn observed at ambient conditions. The crystalline structures of SnO and SnO$_2$ belong to space groups $P4/nmm$ (romarchite) and $P4_2/mnm$ (rutile), respectively [9]. The expected Bragg peak positions in Fig. 3 clearly do not correlate with the crystalline structure of the surface oxide of liquid Sn. Moreover, it is not possible to match these structures to that of Sn surface oxide by lattice parameter adjustment within a reasonable range (variations of up to 20% from nominal values).

There are reported high-pressure modifications of the Sn oxides' structure [10,11]. The transition to these structures occurs at pressures above 21 GPa. The diffraction patterns of these structures are presented in Fig. 3. These patterns also do
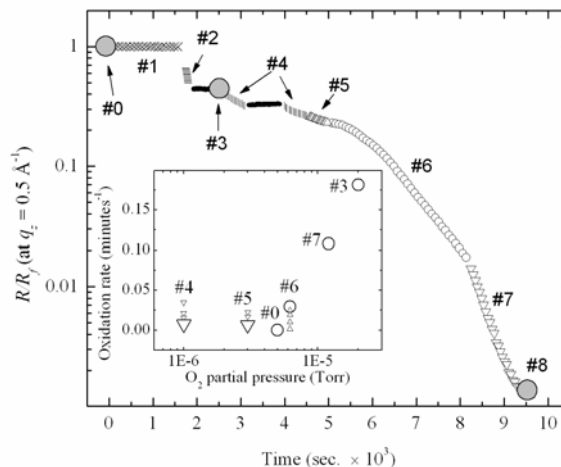

Fig. 2. Fresnel-normalized x-ray reflected intensity at $q_z = 0.5$ Å^{-1} during the oxidation process as a function of time. The inset shows the relative rate of change of the reflected intensity, $\dfrac{1}{R/R_f}\dfrac{d}{dt}\left[\ln(R/R_f)\right]$, which qualitatively reflects the oxidation rate. Circles in the inset denote stable logarithmic rates and triangles represent the rates which are changing with time. Large filled circles in the figure (#0, #3, #8) denote points where complete reflectivity measurements were taken. Other regions are: #1 — oxygen pressures below 5.0×10^{-6} Torr; #2 — 2.0×10^{-5} Torr; #4 — 1.0×10^{-6} Torr; #5 — 3.0×10^{-6} Torr; #6 — 6.2×10^{-6} Torr; #7 — 1.0×10^{-5} Torr; thick solid lines denote regions where oxygen was not applied, but measurements were continued.

not match the peaks experimentally observed for the surface Sn oxide; however, the most significant observation is that the ratio of positions of the two diffraction peaks of the surface oxide is $\sqrt{3}/2$, which is precisely the ratio of the two lowest order peaks for the high-pressure phases. In fact, to the best of our knowledge the face-centered cubic (fcc) lattice is the only one for which the two smallest reciprocal lattice distances are in this ratio. Thus it is not likely that the observed surface oxide is anything other than the fcc structure. The problem with this is that in order to produce the observed surface oxide peaks the lattice parameter must have a value of 4.455 Å which represents a 9% reduction from the published values for the high-pressure structures. At first glance it seems rather implausible; however, the Sn-O closest neighbor distance of this form of the surface oxide is 1.83 Å for the high-pressure phase structure and 2.23 Å for the rock salt structure. The latter precisely matches the molecular Sn-O bond length of the romarchite SnO structure (2.20 Å). On the other hand, since the former is smaller than the molecular Sn-O covalent bond length of 1.95 Å, the rock salt structure may be more realistic. Moreover, the rock salt structure along the [111] crystallographic direction consists of alternating planes of Sn and O atoms with a spacing between two closest Sn planes of 2.57 Å which matches the spacing found between uppermost surface layers of the clean liquid Sn surface of 2.55 Å [3]. A second argument in favor of the rock salt structure is that the (200) to (111) GID peak intensity ratio of the rock salt structure, 0.7, is significantly closer to the experimentally observed ratio, 0.8, than the ratio of peaks of the high-
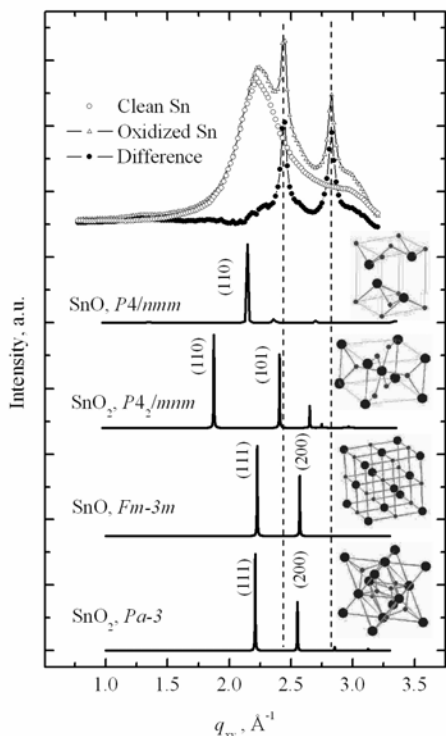
Fig. 3. Grazing Incidence Diffraction (GID) scans of the clean liquid Sn surface and the surface after exposure to a total oxygen dose of 3.1×10^3 L as described in step #3 of Table 1. The difference plot highlights the surface oxide diffraction pattern showing two peaks at $q_{xy} = 2.442$ Å^{-1} and 2.827 Å^{-1}. Positions of the diffraction lines of known SnO and SnO$_2$ structures are shown in the figure along with their crystal models.

pressure phase structure 0.57. Thus, although the density of the fcc form of the Sn-oxide is high, the lattice spacings themselves are not unphysical.

Without measurements of higher order Bragg peaks our interpretation of a high density fcc surface oxide can be considered somewhat speculative. On the other hand, in view of the fact that the only two small angle Bragg peak positions appear in exactly the ratio for the fcc lattices it is very difficult to think of an alternative lattice.

Summary

In the present study we found that the surface of liquid Sn is resistant to oxidation until a threshold oxidation pressure is reached. The oxidation begins within the pressure interval of 3.0×10^{-6} Torr and 6.2×10^{-6} Torr. Above this threshold oxidation pressure a uniform growth of oxide islands on the liquid Sn surface is detected. The islands' surface is very rough and the presence of oxide patches is manifested in a uniform reduction of the specular signal reflected by clean Sn surface.

The diffraction pattern associated with the surface oxide does not match any of the known Sn oxide phases. On the other hand, the appearance of only two Bragg peaks whose scattering vectors are in the ratio of $\sqrt{3}/2$, and with the observed intensities is an unambiguous signature of the fcc structure. It is troublesome that the calculated density for this

fcc phase is 50% to 80% higher than that of the published Sn oxide phases; however, we have not been able to construct an alternative identification. It would be very useful to extend the GID measurement to search for higher wave-vector Bragg peaks.

These observations raise the question of whether the structures that form in a chemical reaction at the surfaces of a liquid metal are fundamentally different from those that form in a bulk chemical reaction, or at the surface of a crystal. For example, we do yet not know the structure of oxides that form on the various facets of a Sn crystal. Are any of them similar to the surface oxide that forms on liquid Sn? Secondly, is the anomalous surface oxide on liquid Sn an indicator that anomalous oxides will also form on the surfaces of other liquid metals? We know that the surface oxide on liquid Ga is amorphous but we do not know if the rough oxide that forms on the surface of liquid In is crystalline or not. This is clearly an area that requires further study. From a theoretical perspective there is a compelling need to ask why this particular cubic phase is favored by the surface over the "normal" structures of the oxides.

Acknowledgements

References

[1] H. Schmalzried, Chemical Kinetics of Solids, Weinheim, VCH Verlagsgesellschaft, 1995.
[2] C. Schuessler-Langeheine, R. Meier, H. Ott, Z. Hu, C. Mazumdar, G. Kaindl, E. Weschke, Phys. Rev. B 60, 3449 (1999).
[3] O.G. Shpyrko, A. Grigoriev, C. Steimer, P.S. Pershan, B.M. Ocko, M. Deutsch, B. Lin, M. Meron, T. Graber, J. Gebhardt, Phys. Rev. B 70, 224206 (2004).
[4] H. Tostmann, E. DiMasi, P.S. Pershan, B.M. Ocko, O.G. Shpyrko, M. Deutsch, Phys. Rev. B 59, 783 (1999).
[5] M.J. Regan, H. Tostmann, P.S. Pershan, O.M. Magnussen, E. DiMasi, B.M. Ocko, M. Deutsch, Phys. Rev. B 55, 10786 (1997).
[6] E. Ricci, L. Nanni, A. Passerone, Phil. Trans. R. Soc. Lond. A 356, 857 (1998).
[7] Y.L. Wang, S.J. Lin, Phys Rev B 53, 6152 (1996).
[8] Y. Waseda, The Structure of Non-Crystalline Materials: Liquids and Amorphous Solids, New York, McGraw-Hill, 1980.
[9] M. Meyer, G. Onida, M. Palummo, L. Reining, Phys. Rev. B 64, 045119 (2001).
[10] L. Liu, Science 199, 422 (1978).
[11] J. Haines, Science 271, 629 (1996).